Communicative & Integrative Biology 6:6, e27315; November/December; © 2013 Landes Bioscience

Interactions between intercellular adhesion molecule-5 positive elements and their surroundings in the rodent visual cortex

Emily A Kelly[1], Marie-Ève Tremblay[1,†], Carl G Gahmberg[2], Li Tian[3], Ania K Majewska[1,*]

[1]Neurobiology & Anatomy; University of Rochester; Rochester, NY USA; [2]Department of Bioscience; University of Helsinki; Helsinki, Finland; [3]Neuroscience Center; University of Helsinki; Helsinki, Finland

[†]Current affiliation: Department of Molecular Medicine; Université Laval; Québec City, QC Canada

The telencephalon-associated intercellular adhesion molecule 5 (Telencephalin; ICAM-5) regulates dendritic maturation, a process dependent on extracellular proteases in the developing brain. Using transmission electron microscopy, we have reported previously that ICAM-5 is localized primarily in dendritic protrusions during a period of robust synaptogenesis (P14 in mouse visual cortex). As dendritic protrusions mature (P28), ICAM-5 immuno-reactivity shifts from dendritic protrusions into dendritic shafts. ICAM-5 immuno-reactivity does not shift in animals lacking the matrix metalloproteinase-9 (MMP-9), a protease shown to regulate ICAM-5 cleavage. Cleaved ICAM-5 (soluble fraction; sICAM-5) has been shown to bind to a number of receptors located in neighboring structures, resulting in a variety of downstream signaling events, including enhanced neurotransmission. Here, we investigated the potential MMP-regulated ICAM-5 signaling by examining the relationship between ICAM-5 immuno-positive elements and the structures that directly neighbor them.

Keywords: Telencephalin, ICAM-5, electron microscopy, mouse, visual cortex, ultrastructural

*Correspondence to: Ania K Majewska; Email: Ania_Majewska@urmc.rochester.edu

Submitted: 10/17/2013

Revised: 11/21/2013

Accepted: 11/22/2013

Citation: Kelly EA, Tremblay M, Gahmberg CG, Tian L, Majewska AK. Interactions between intercellular adhesion molecule-5 positive elements and their surroundings in the rodent visual cortex. Communicative & Integrative Biology 2013; 6:e27315; http://dx.doi.org/10.4161/cib.27315

Kelly EA, Tremblay ME, Gahmberg CG, Tian L, Majewska AK. The subcellular localization of intercellular adhesion molecule-5 (telencephalin) in the visual cortex is not developmentally regulated in the absence of matrix metalloproteinase-9. J Comp Neurol 2013 http://dx.doi.org/10.1002/cne.23440

The intercellular adhesion molecule 5 (ICAM-5; Telencephalin) is a dendrite-specific cell adhesion molecule[1,2] postulated to regulate dendritic morphology and function. ICAM-5 is cleaved by multiple matrix metalloproteinases (MMPs) including MMP-2, -9[3] as well as MMP-3, -7.[4,5] Both the cleaved product (soluble ICAM-5, sICAM-5) and remaining transmembrane ICAM-5 fragment have been implicated in varying downstream effects.[6] For instance, MMP-2 and -9 mediated cleavage of ICAM-5 results in both filopodial elongation and spine maturation[3,4] and sICAM-5 has been shown to interact with receptor complexes on neighboring structures both pre- and postynaptically.[3-5,7-10] Previously, we used immunocytochemical electron microscopy (EM) to determine ICAM-5 expression and localization within the neuropil in vivo in mice with and without MMP-9 expression. Our results confirm previous reports showing postsynaptic expression of ICAM-5 and additionally reveal an unexpected expression in glia. We also show changes in ICAM-5 expression in MMP-9 null animals suggesting a role for this extracellular protease in the developmental processing of ICAM-5. Here we extend these findings to show that ICAM-5 expressing elements preferentially contact synaptic structures, regardless of MMP-9 expression. These findings shed light on the possible modes of ICAM-5 signaling in the developing brain.

We identified and quantified the structures that surround ICAM-5 labeled profiles in wildtype (WT; **Figure 1**) and MMP-9 knockout (KO) mouse visual cortex (**Fig. 2**) using immnoperoxidase staining and electron microscopic analysis. Classification of labeled ICAM-5 (+) structures and their surrounding elements has been previously described (**Fig. 1A**; see ref. 11). At P14, ICAM-5 labeled

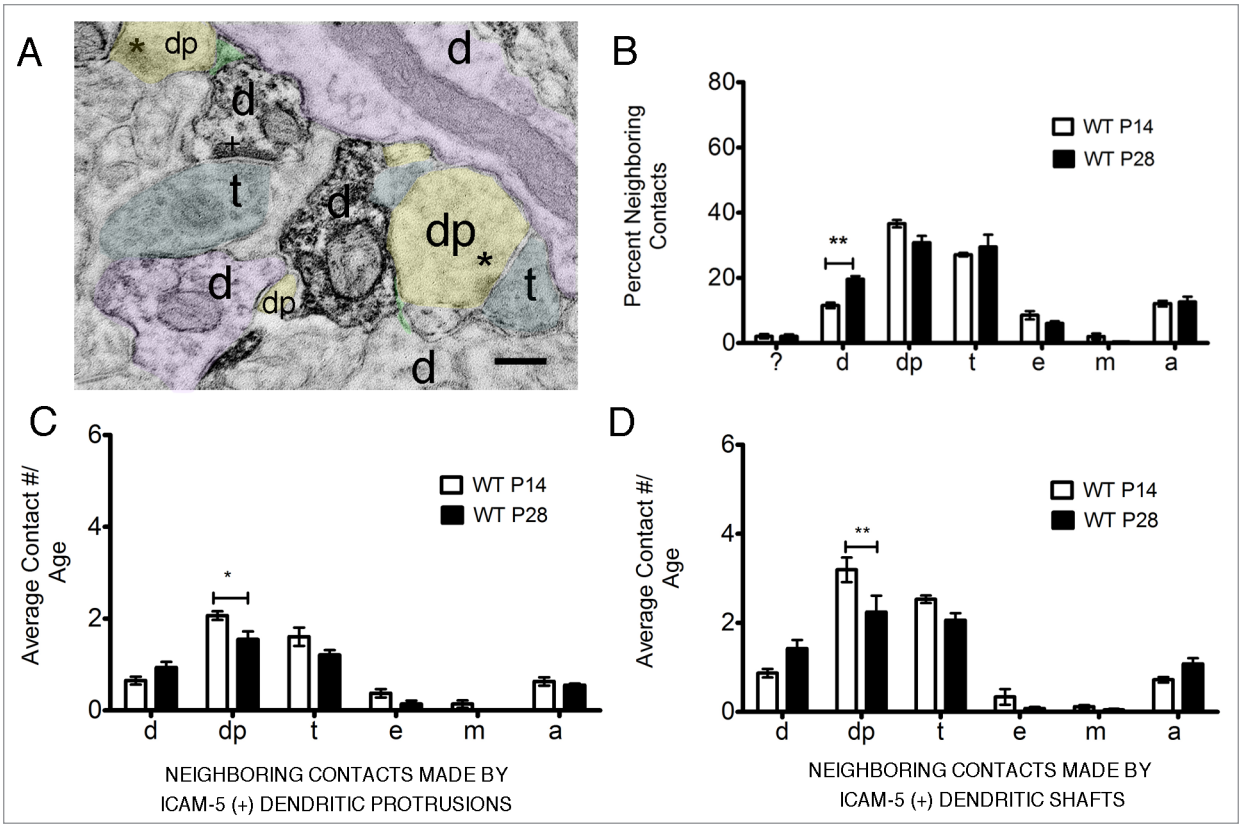

Figure 1. Quantitative analysis of neighboring contacts made onto ICAM-5 labeled elements in WT P14 and P28 mouse visual cortex. (**A**) Anti-ICAM-5 immunoperoxidase reactivity at P28 in WT mouse visual cortex denoting the identification of neighboring contacts. (**B**) The percent of neighboring contacts onto ICAM-5 labeled elements show a high proportion of dendritic protrusions and axon terminal contacts at P14. By P28, there is a significant increase in dendritic shaft contacts. (**C**) The average number of contacts onto labeled dendritic protrusions at P14 and P28 in WT mice. (**D**) The average number of contacts onto labeled dendritic shafts at P14 and P28 in WT mice. Scale bar = (A) 200 nm. Labeling index = axon terminals (blue), dendritic shafts (purple), dendritic protrusions (yellow), astrocytes (green). Abbreviations: ?, unknown/ unidentifiable element; d, dendrite; dp, dendritic protrusions; t, terminal; e, extracellular space; m, microglia; a, astrocyte. * = $P < 0.05$, ** = 0.01, *** = $P < 0.001$, **** = $P < 0.0001$.

structures were contacted by dendritic protrusions (dp; 37% of all interacting structures), axonal terminals (t; 27%), and dendrites (d; 12%), as well as astrocytes (a; 12%). ICAM-5 labeled structures were rarely contacted by microglial processes (m; 2%) possibly due to the low density of these dynamic structures in the neuropil or to the difficulty in identifying them positively without immunostaining for a microglial marker (**Fig. 1B**). At P28, ICAM-5 immunopositive elements had similar contacts, however, there were significantly more neighboring dendrites (20%; Two-way ANOVA; Bonferronni multiple comparisons; $P < 0.01$).

ICAM-5 immunoreactivity was predominantly found in dendritic protrusions and dendritic shafts from P14 to P28 in WT mice.[11] We sought to investigate the relationship between these specific profiles and their neighboring contacts (**Fig. 1C-D**). At P14, ICAM-5 labeled dendritic protrusions and dendrites behaved similarly and made preferential contacts with dendritic protrusions and axon terminals (One-way ANOVA, Bonferroni multiple comparisons, $P < 0.05$–0.001), although labeled dendrites made significantly more contacts with dendritic protrusions ($P < 0.001$; Two-way ANOVA, Bonferroni multiple comparisons) and axonal terminals ($P < 0.01$; Two-way ANOVA, Bonferroni multiple comparisons; **Figure 1C and 1D**; WT P14 "dp" contacts vs "d" contacts) than did dendritic protrusions. By P28 both dendritic protrusions and dendrites had significantly fewer contacts with dendritic protrusions than at P14, but not with axonal terminals ("dp" contacts = $P < 0.05$; "d" contacts = $P < 0.01$; **Figure 1C–D**).

We next assessed the profile of neighboring contacts to ICAM-5 immunopositive elements in MMP-9 KO cortex (**Fig. 2**). Whereas in WT mice we noted a significant increase in ICAM-5-immunoreactive elements making contact with dendrites at P28 compared with P14 (**Fig. 1B**), we instead found a significant increase in axonal terminal contact and a decrease in astrocytic contact between P14 and P28 in MMP-9 KO mice (**Fig. 2A**). The contact profiles for individual elements at P14 (**Fig. 2B**) and P28 (**Fig. 2C**) were however similar to those observed in WT mice (**Fig. 1C and 1D**); all immunoreactive dendritic protrusions and dendrites made preferential contacts with dendritic protrusions and axon terminals at both ages and this effect was more pronounced for dendrites than dendritic protrusions. The decrease in contact with dendritic

protrusions at P28 seen in the WT animals was not observed in MMP-9 KOs.

We have shown previously that ICAM-5 immunoreactivity is found preferentially in dendritic protrusions during early development and is redistributed to the dendritic shaft as the dendrite matures.[11] ICAM-5 cleavage is regulated by MMPs whereby the ICAM-5 ectodomain is shed and binding to neighboring substrates triggers downstream signaling events.[3-5,7,8,10,12] Understanding the ultrastructural environment surrounding ICAM-5 immuno-positive structures could shed light on preferential signaling partners for ICAM-5 expressing structures. We found small changes in the elements that contacted ICAM-5 immunolabeled structures during the time that ICAM-5 is developmentally regulated. At P14, when ICAM-5 immunoreactivity is most prevalent in dendritic protrusions, these elements are contacted preferentially by axon terminals and neighboring protrusions. As the brain develops, ICAM-5 labeled elements are largely surrounded by dendritic shafts as well as axonal terminals and dendritic protrusions suggesting additional potential developmental partners for extracellular ICAM-5 signaling. These changes are small in magnitude and the consistency of the environs of ICAM-5 labeled structures, despite shifting ICAM-5 expression and on-going brain development, suggests a relatively uniform set of signaling partners for ICAM-5. The apposition of ICAM-5 labeled elements with dendritic and axonal profiles may allow binding to the α5β1 integrin in both pre and postsynaptic membranes,[9] leading to synaptic maturation. sICAM-5 may also have a role in activating this pathway.[4,9]

In the absence of MMP-9, ICAM-5 immuno-reactive elements make significantly more contacts with axonal terminals. This is especially apparent at later time points (P28) when presumed uncleaved ICAM-5 remains in dendritic protrusions rather than redistributing to dendritic shafts.[11] Recent findings suggest that ICAM-5 might associate with presynaptically located β1 integrin during early phases of synapse formation (nascent synapses).[9] Furthermore, it is thought that the ICAM-5/ β1 integrin interaction at this junction may promote filopodial elongation or maintain the morphology of thin protrusions before they develop into mature spines.[9] In the absence of MMP-9, the enhanced apposition of presynaptic elements may be due to such an interaction which maintains synapses in an immature state or serve a compensatory role increasing pre and postsynaptic associations.

As a technical consideration, it is important to note that immunoperoxidase staining was chosen for this analysis considering its exceptional sensitivity of immunodetection, compared with immunogold labeling.[13] Because of the diffusion of the DAB product, this

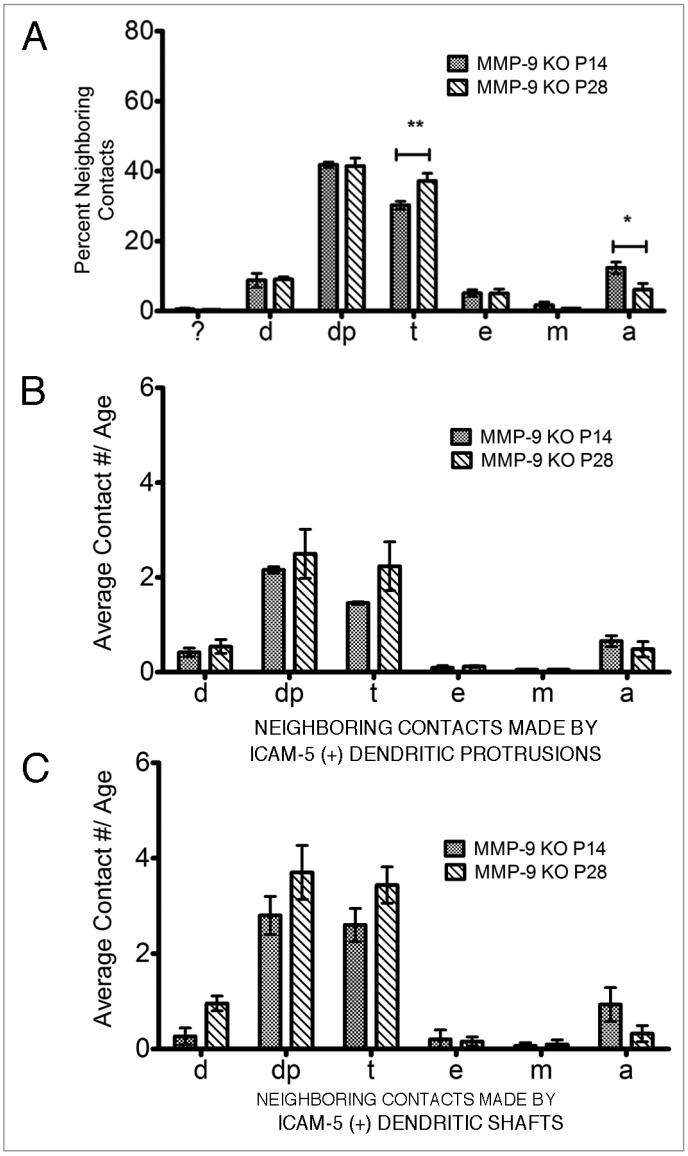

Figure 2. Quantitative analysis of neighboring contacts made onto ICAM-5 labeled elements in MMP-9 KO P14 and P28 mouse visual cortex (**A**) The percent of neighboring contacts onto ICAM-5 labeled elements showed a high proportion of dendritic protrusions and terminal contacts at P14 and P28. (**B**) The average number of contacts onto immunoreactive dendritic protrusions at P14 and P28 in MMP-9 KO mice. (**C**) The average number of contacts onto immunoreactive dendritic shafts at P14 and P28 in MMP-9 KO mice. A total of 3 animals (1,000 μm^2 of neuropil/animal) at P14 (~200 elements/animal) and P28 (~200 elements/animal) were analyzed. Abbreviations: ?, unknown/ unidentifiable element; d, dendrite; dp, dendritic protrusions; t, terminal; e, extracellular space; m, microglia; a, astrocyte. ** = 0.01, **** = $P < 0.0001$.

analysis is not necessarily indicative of direct contact between ICAM-5 and surrounding structures, but instead gives an idea of the environment of ICAM-5 labeled elements. Future experiments, implementing immunogold dual labeling for ICAM-5 and potential binding/signaling partners, are necessary. These preliminary data are informative, however, because they suggest that as ICAM-5 expressing dendrites and protrusions mature their extracellular environment remains similar.

Material and Methods

Method details can be found in ref. 11. Briefly, 40,000X pictures were taken in layer II of V1 in 3 animals per condition at the tissue-resin border (total surface ~1,000 μm2 of neuropil per animal). To determine the average number of contacts made per ICAM-5 labeled element we calculated the total number of contacts with individual labeled element types per animal and divided that number by the total labeled element number. This was averaged across all animals in each condition.

Cellular profiles were identified using criteria previously defined in single-ultrathin sections[15,20-22] as outlined below. Subcellular profiles that were difficult to identify were labeled "unknown." *Dendrites* had irregular contours, elongated mitochondria in parallel with their central axis, frequent protuberances and synaptic contacts with axon terminals. Transverse dendrites showed rounded morphology, mitochondria, microtubules, and a larger diameter than unmyelinated axons. *Dendritic protrusions* often protruded from dendritic shafts, displayed rounded morphologies, no mitochondria, and sometimes contained electron-dense accumulations (postsynaptic densities) at synaptic contact sites with axon terminals. *Axon terminals* included 40 nm diameter synaptic vesicles, contained mitochondria, had rounded to elongated morphologies and synaptic contacts with dendritic shafts and protrusions. *Astrocytes* were electron-lucent structures encasing other elements. *Microglial* processes displayed irregular contours with obtuse angles, distinctive long stretches of endoplasmic reticulum, electron-dense cytoplasm, numerous large vesicles, occasional multi-vesicular bodies, vacuoles or cellular inclusions, and distinctive surrounding extracellular space.[21-23]Glial structures were grouped into one category for this study.

Disclosure of Potential Conflicts of Interest

No potential conflicts of interest were disclosed.

References

1. Yoshihara Y, Mori K. Telencephalin: a neuronal area code molecule? Neurosci Res 1994; 21:119-24; PMID:7724062; http://dx.doi.org/10.1016/0168-0102(94)90153-8
2. Yoshihara Y, Oka S, Nemoto Y, Watanabe Y, Nagata S, Kagamiyama H, Mori K. An ICAM-related neuronal glycoprotein, telencephalin, with brain segment-specific expression. Neuron 1994; 12:541-53; PMID:7794412; http://dx.doi.org/10.1016/0896-6273(94)90211-9
3. Tian L, Stefanidakis M, Ning L, Van Lint P, Nyman-Huttunen H, Libert C, Itohara S, Mishina M, Rauvala H, Gahmberg CG. Activation of NMDA receptors promotes dendritic spine development through MMP-mediated ICAM-5 cleavage. J Cell Biol 2007; 178:687-700; PMID:17682049; http://dx.doi.org/10.1083/jcb.200612097
4. Conant K, Lonskaya I, Szklarczyk A, Krall C, Steiner J, Maguire-Zeiss K, Lim ST. Methamphetamine-associated cleavage of the synaptic adhesion molecule intercellular adhesion molecule-5. J Neurochem 2011; 118:521-32; PMID:21166806; http://dx.doi.org/10.1111/j.1471-4159.2010.07153.x
5. Conant K, Wang Y, Szklarczyk A, Dudak A, Mattson MP, Lim ST. Matrix metalloproteinase-dependent shedding of intercellular adhesion molecule-5 occurs with long-term potentiation. Neuroscience 2010; 166:508-21; PMID:20045450; http://dx.doi.org/10.1016/j.neuroscience.2009.12.061
6. Furutani Y, Matsuno H, Kawasaki M, Sasaki T, Mori K, Yoshihara Y. Interaction between telencephalin and ERM family proteins mediates dendritic filopodia formation. J Neurosci 2007; 27:8866-76; PMID:17699668; http://dx.doi.org/10.1523/JNEUROSCI.1047-07.2007
7. Lonskaya I, Partridge J, Lalchandani RR, Chung A, Lee T, Vicini S, Hoe HS, Lim ST, Conant K. Soluble ICAM-5, a product of activity dependent proteolysis, increases mEPSC frequency and dendritic expression of GluA1. PLoS One 2013; 8:e69136; PMID:23844251; http://dx.doi.org/10.1371/journal.pone.0069136
8. Niedringhaus M, Chen X, Dzakpasu R, Conant K. MMPs and soluble ICAM-5 increase neuronal excitability within in vitro networks of hippocampal neurons. PLoS One 2012; 7:e42631; PMID:22912716; http://dx.doi.org/10.1371/journal.pone.0042631
9. Ning L, Tian L, Smirnov S, Vihinen H, Llano O, Vick K, Davis RL, Rivera C, Gahmberg CG. Interactions between ICAM-5 and β1 integrins regulate neuronal synapse formation. J Cell Sci 2013; 126:77-89; PMID:23015592; http://dx.doi.org/10.1242/jcs.106674
10. Tian L, Nyman H, Kilgannon P, Yoshihara Y, Mori K, Andersson LC, Kaukinen S, Rauvala H, Gallatin WM, Gahmberg CG. Intercellular adhesion molecule-5 induces dendritic outgrowth by homophilic adhesion. J Cell Biol 2000; 150:243-52; PMID:10893271; http://dx.doi.org/10.1083/jcb.150.1.243
11. Kelly EA, Tremblay ME, Gahmberg CG, Tian L, Majewska AK. The subcellular localization of intercellular adhesion molecule-5 (telencephalin) in the visual cortex is not developmentally regulated in the absence of matrix metalloproteinase-9. J Comp Neurol 2013; PMID:23897576; http://dx.doi.org/10.1002/cne.23440
12. Tian L, Lappalainen J, Autero M, Hänninen S, Rauvala H, Gahmberg CG. Shedded neuronal ICAM-5 suppresses T-cell activation. Blood 2008; 111:3615-25; PMID:18223167; http://dx.doi.org/10.1182/blood-2007-09-111179
13. Tremblay ME, Riad M, Bouvier D, Murai KK, Pasquale EB, Descarries L, Doucet G. Localization of EphA4 in axon terminals and dendritic spines of adult rat hippocampus. J Comp Neurol 2007; 501:691-702; PMID:17299751; http://dx.doi.org/10.1002/cne.21263
14. Bouvier D, Corera AT, Tremblay ME, Riad M, Chagnon M, Murai KK, Pasquale EB, Fon EA, Doucet G. Pre-synaptic and post-synaptic localization of EphA4 and EphB2 in adult mouse forebrain. J Neurochem 2008; 106:682-95; PMID:18410519; http://dx.doi.org/10.1111/j.1471-4159.2008.05416.x
15. Tremblay ME, Riad M, Chierzi S, Murai KK, Pasquale EB, Doucet G. Developmental course of EphA4 cellular and subcellular localization in the postnatal rat hippocampus. J Comp Neurol 2009; 512:798-813; PMID:19086003; http://dx.doi.org/10.1002/cne.21922
16. Bouvier D, Tremblay ME, Riad M, Corera AT, Gingras D, Horn KE, Fotouhi M, Girard M, Murai KK, Kennedy TE, et al. EphA4 is localized in clathrin-coated and synaptic vesicles in adult mouse brain. J Neurochem 2010; 113:153-65; PMID:20067584; http://dx.doi.org/10.1111/j.1471-4159.2010.06582.x
17. Kelly EA, Majewska AK. Chronic imaging of mouse visual cortex using a thinned-skull preparation. Journal of visualized experiments: JoVE 2010.
18. Tremblay ME, Riad M, Majewska A. Preparation of mouse brain tissue for immunoelectron microscopy. Journal of visualized experiments: JoVE 2010.
19. Mortillo S, Elste A, Ge Y, Patil SB, Hsiao K, Huntley GW, Davis RL, Benson DL. Compensatory redistribution of neuroligins and N-cadherin following deletion of synaptic β1-integrin. J Comp Neurol 2012; 520:2041-52; PMID:22488504; http://dx.doi.org/10.1002/cne.23027
20. Peters A, Palay S, Webster H. The fine structure of the nervous system: The neurons and supporting cells. Philadelphia: W.B. Saunders, 1991.
21. Lu SM, Tremblay ME, King IL, Qi J, Reynolds HM, Marker DF, Varrone JJ, Majewska AK, Dewhurst S, Gelbard HA. HIV-1 Tat-induced microgliosis and synaptic damage via interactions between peripheral and central myeloid cells. PLoS One 2011; 6:e23915; PMID:21912650; http://dx.doi.org/10.1371/journal.pone.0023915
22. Tremblay ME, Lowery RL, Majewska AK. Microglial interactions with synapses are modulated by visual experience. PLoS Biol 2010; 8:e1000527; PMID:21072242; http://dx.doi.org/10.1371/journal.pbio.1000527
23. Tremblay ME, Zettel ML, Ison JR, Allen PD, Majewska AK. Effects of aging and sensory loss on glial cells in mouse visual and auditory cortices. Glia 2012; 60:541-58; PMID:22223464; http://dx.doi.org/10.1002/glia.22287